Space Charge Modelling in HVDC Extruded Cable Insulation

Yunpeng **ZHAN** University of Southampton, (United Kingdom), yz10n16@soton.ac.uk

George **CHEN**, University of Southampton, (United Kingdom), gc@ecs.soton.ac.uk

Ying **LIU** Xi'an Jiaotong University, (China), candyly@mail.xjtu.edu.cn

ABSTRACT

In this paper, a bipolar charge transport model was applied to simulate the space charge behaviour within the HVDC cable polymeric insulation. Based on many experimental observations, a threshold electric field at which the charge injection takes place was introduced to the model. Considering the practical operation of HVDC cables, a transient temperature distribution across the insulation was implemented to compute the charge generation and transportation processes. The simulations results suggest that the thermal transient has a significant effect on charge dynamics in the cable.

KEYWORDS

Bipolar transport, HVDC, polymeric insulation, thermal transient.

INTRODUCTION

HVDC cables are playing an important role in undersea power transmission and offshore renewable energy integration due to its significant advantages, such as lower energy losses and higher reliability [1]. It is widely believed that traditional cables (oil-filled cable and mass-impregnated cable) can pose a risk of environmental pollution in case of an accident [2]. Therefore, polymeric material, notably cross-linked polyethylene (XLPE), has been used as the main insulation material for HVDC cables due to its economical production, environmental benefits, and electrical properties. However, the main drawback of extruded cables is the impact caused by space charge phenomena [3]. The accumulated space charge can distort the electric field distribution in the insulation, leading to accelerated aging and eventual breakdown [4]. Particularly, after polarity reversal, the presence of space charge can give a considerable electric field enhancement, which is usually unacceptable and easily cause permanent failure in the insulation [5]. Issues related to space charge behaviour need to be further studied, in order to enhance the reliability and lifetime of extruded HVDC cables.

During the recent decades, extensive experimental efforts have been made to investigate the characteristics of space charge in order to understand the relationship between space charge and electrical performance of dielectrics [6]. It has been proven that space charge density and movement are dependent on multiple factors, such as the amplitude and duration of the applied electric field, temperature, moisture content, interface condition between conductor and polymer, geometry of the polymer and material properties. Many numerical models have been proposed to simulate the space charge behaviour in polymeric materials, aiming to predict the material behaviour and answer the issues related to charge transport mechanism [7]. The simulation results from these models, when compared with the experimental results, can present reasonable charge density profiles in the bulk of dielectrics and their evolving with time. Many researchers have improved these models in order to achieve a better fit with experimental data and aid to understand the charge dynamics in solid dielectrics [8]. The generation of charge carriers at the electrodes, charge transport process (including charge trapping and detrapping) and charge recombination are considered in these models, and most attempts have been made to describe the charge dynamics characteristics in the planar sample [9]. So far, fewer researchers take into account the cable geometry factor in their models, which have a great impact on the electric field distribution in the insulation. Additionally, the real temperature gradient across the insulation also needs to be considered, because it will affect the charge generation and transport processes greatly. In 2016, S. Le Roy et al proposed an evolution of the bipolar charge transport model within a cylindrical configuration, and a temperature gradient under the steady state is taken into account [10]. The simulated results show how the geometry and the temperature can respectively affect the charge densities and electric field distributions. However, in the real case, when the electrical power transmits through the cable, the heat generated from the conductor due to joule loss will transfer into the cable insulation and outer screen gradually. The temperature gradient across the insulation should vary with time, and this transient temperature state needs to be taken into account. Therefore, a more complex model needs to be developed when considering the thermal effects caused by the flowing current in the conductor.

In the present paper, we proposed a modified bipolar charge transport model to simulate space charge behaviours in a cylindrical cable geometry insulation, which involves the charge carriers generation and transport mechanisms. Compared with the previous work, a threshold electric field is introduced into the model to redefine the charge injection from the electrodes, making it more physically reasonable. Moreover, a transient temperature distribution across the insulation, calculated by means of Fourier's heat diffusion equation, is taken into account to replace the previous steady temperature gradient, aiming to make the simulated results from the model more useful for practical HVDC cable applications.

BRIEF SUMMARY OF THE MODEL

Compared with cross-linked polyethylene (XLPE), the low-density polyethylene (LDPE) is considered being free of additives, which also has the basic properties of cross-

Close and Return

linked polyethylene and well defined chemical structure. It is a simple objective to investigate the charge generation without considering the ionization processes, and thus, we use LDPE as the insulation material. The bipolar charge transport model starts from the injection of positive and negative charge carriers at the interface between insulation and electrodes when the applied electric field exceeds the threshold field. The injected electrons and holes move into the bulk of dielectrics towards the opposite electrodes under the influence of the electric field hence come the conduction current. The trap energy levels localized in the band-gap of the dielectrics. Shallow traps originated by physical defects and deep traps caused by chemical defects in the molecules can capture the mobile carriers and form trapped carriers inside [11]. Therefore, there are four species considered in the model, mobile electron/holes, trapped electrons/holes, as shown in Figure 1.

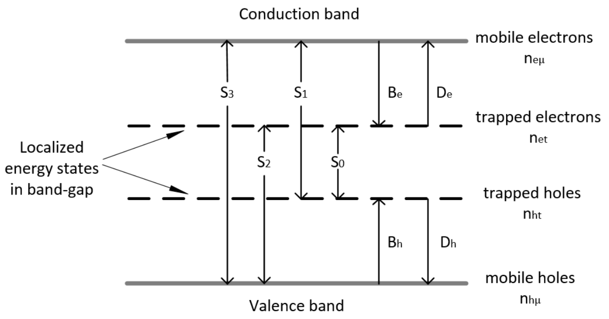

Fig. 1: Schematic representation of the bipolar charge transport model. S_i, B_i and D_i are recombination, trapping and de-trapping coefficients respectively. n_i is the charge density. Indexes e and h refer to electrons and holes; μ ant t refer to mobile and trapped charge carriers [9]**.**

Figure 2 shows the cable geometry and its discretization grid used for the simulation. For the numerical computation, the thickness of the LDPE sample is divided into 200 divisions of different sizes of thickness Δx. In order to optimize the simulation results, the Δx is set to be tightened close to the electrodes. The smallest cell Δx next to the electrodes is of the order of 550 nm, and the maximal is about 100 times as thick as the smallest one.

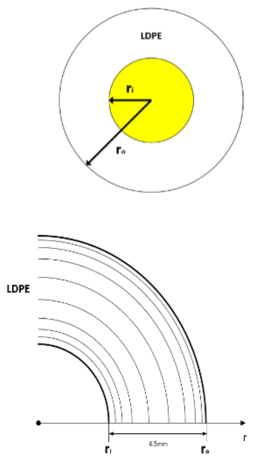

Fig. 2: The schematic representation of the cable geometry and the 1-dimensional grid used for the simualtion.

To describe dynamics of charge accumulation in the polyethylene insulation, three essential space and time dependent equations are presented in cylindrical geometry as following, neglecting diffusion.

Gauss's Law:

$$\frac{\partial^2 V(r,t)}{\partial r^2} + \frac{1}{r}\frac{\partial V(r,t)}{\partial r} = -\frac{\rho(r,t)}{\varepsilon_0 \varepsilon_r} \qquad (1)$$

Continuity equation:

$$\frac{\partial n_{a\mu,at}(r,t)}{\partial t} + \frac{1}{r}\frac{\partial (j_a \times r)}{\partial r} = s_{a\mu,at}(r,t) \qquad (2)$$

Ohmic's Law:

$$j_a(r,t) = \mu_a(r,t) n_{a\mu}(r,t) E(r,t) \qquad (3)$$

where j_a is the conduction current density; n is the charge density; E is the electric field; ρ is the net charge density; ε_0 is the vacuum permittivity, ε_r is the relative dielectric permittivity, which is considered as a constant (2.3 for polyethylene). Here a refers to the type of charge, and the subscript μ or t refers respectively to mobile or trapped charge. S are the source terms, which encompass the changes in local density by processes other than transport (trapping, detrapping and recombination).

The continuity equation is solved by using a splitting method, and the source term equation actually consists of four equations for each species.

$$s_1 = \frac{\partial n_{e\mu}}{\partial t} = -S_1 n_{ht} n_{e\mu} - S_3 n_{h\mu} n_{e\mu} - B_e n_{e\mu}\left(1 - \frac{n_{et}}{n_{oet}}\right) + D_e n_{et}$$

$$s_2 = \frac{\partial n_{h\mu}}{\partial t} = -S_2 n_{et} n_{h\mu} - S_3 n_{h\mu} n_{e\mu} - B_h n_{h\mu}\left(1 - \frac{n_{ht}}{n_{oht}}\right) + D_h n_{ht}$$

$$s_3 = \frac{\partial n_{et}}{\partial t} = -S_2 n_{h\mu} n_{et} - S_0 n_{ht} n_{et} + B_e n_{e\mu}\left(1 - \frac{n_{et}}{n_{oet}}\right) - D_e n_{et}$$

$$s_4 = \frac{\partial n_{ht}}{\partial t} = -S_1 n_{ht} n_{e\mu} - S_0 n_{ht} n_{et} + B_h n_{h\mu}\left(1 - \frac{n_{ht}}{n_{oht}}\right) - D_h n_{ht} \qquad (4)$$

where s_1, s_2, s_3 and s_4 are the source terms for each species; S_0, S_1, S_2 and S_3 are the recombination coefficients for different opposite species; B_e and B_h are the trapping coefficients for electrons/holes; $n_{e\mu}$, n_{et}, $n_{h\mu}$ and n_{ht} respectively indicate the densities of each species; n_{oet} and n_{oht} are the trap densities for electrons and holes. D_e and D_h are the detrapping coefficients for electrons and holes of the form [10]:

$$D_{e,h}(r,t) = v * exp\left(\frac{-e * w_{tre,trh}}{k_B T(r)}\right) \qquad (5)$$

Conduction between shallow traps is described using a temperature-dependent hopping type mobility of the form, for each kind of carrier:

$$\mu_{e,h}(r,t) = \frac{2dv}{E(r,t)} \exp\left(\frac{-ew_{\mu e,\mu h}}{k_B T(r)}\right) \sinh\left(\frac{eE(r,t)d}{2k_B T(r)}\right) \qquad (6)$$

where d is the distance between traps; e is the elementary charge; T is the temperature inside the dielectric, function of radius; k_B is the Boltzmann's constant; w is the hopping barrier height for electrons and holes respectively. v is the attempt to escape frequency, of the form:

$$v = k_B T(r)/h \qquad (7)$$

where h is the Planck constant, 6.626×10^{-34}(J·s).

The charge carriers recombination is accounted for considering different coefficients S_i for several electron-hole pairs. These coefficients are of the Langevin form [12], function of the carrier mobility, hence function of temperature, can be written as follows:

$$S_0 = 0$$
$$S_1 = S_{e\mu,ht}(r,t) = \frac{\mu_e(r,t)}{\varepsilon_0 \varepsilon_r}$$
$$S_2 = S_{et,h\mu}(r,t) = \frac{\mu_h(r,t)}{\varepsilon_0 \varepsilon_r}$$
$$S_3 = S_{e\mu,h\mu}(r,t) = \frac{\mu_e(r,t)+\mu_h(r,t)}{\varepsilon_0 \varepsilon_r} \quad (8)$$

The injection of charge carriers occurs at the interface between the conductor and the insulator when the applied electric field is higher than the threshold field. From the previous work done by G Mazzanti et al [13], a value of threshold electric field about 10 kV/mm has been identified for charge injection in polyethylene. In this study, when the applied field exceeds the critical value (10 kV/mm), the boundary condition is defined by the Schottky injection at both electrodes.

$$j_e(r_o,t) = AT^2(r) exp\left(\frac{-ew_{ei}}{k_B T(r)}\right) exp\left(\frac{e}{k_B T(r)}\sqrt{\frac{eE(r,t)}{4\pi\varepsilon_0\varepsilon_r}}\right)$$
$$j_h(r_i,t) = AT^2(r)\, exp\left(\frac{-ew_{hi}}{k_B T(r)}\right) exp\left(\frac{e}{k_B T(r)}\sqrt{\frac{eE(r,t)}{4\pi\varepsilon_0\varepsilon_r}}\right) \quad (9)$$

However, there are still few injected space charges can be detected when the bulk is subjected to relatively low electric field. Because of the thermionic effect, thermionic emission and thermionic-field emission also contribute to charge injection. These injected charge carriers can be regarded to be caused by the ohmic conduction at the interface between metal and dielectrics. For sake of simplification, these emissions are considered as a linear field-dependent function.

$$J = \sigma E = \mu n q E \quad (10)$$

It should be noted that the extraction barriers of charge carriers are not considered, and the extraction fluxes for holes at the cathode and for electrons at the anode follow the transport equation. The time step Δt in the simulation must satisfy the Courant-Friedrich-Levy relation (CFL), involving that the charge displacement within Δt is less than the size Δx, and is calculated automatically to be less than the quickest phenomenon occurring in the dielectric, including trapping, detrapping and recombination.

SIMULATION RESULTS

Simulations have been performed on a medium voltage cable, the inner radius (r_i) is 4.5mm, the outer radius (r_o) is 9mm, giving an insulation thickness of 4.5mm. A positive voltage of 90 kV is applied at the inner electrode and the average electric field inside the dielectric is about 20 kV/mm. The parameters used in the simulation are given in Table 1, and these are mostly the ones that have been optimized from measurements achieved on space charge for a plane parallel LDPE [9].

Table 1: Parameters used for the simulations

Parameter	Value	Unit
Injection barrier heights W_{ei} for electrons W_{hi} for holes	 1.27 1.16	 eV eV
Trapping coefficients B_e for electrons B_h for holes	 0.05 0.05	 s^{-1} s^{-1}
Trap depths (for mobility) $w_{\mu e}$ for electrons $w_{\mu h}$ for holes	 0.71 0.65	 eV eV
Trap densities n_{oet} for electrons n_{oht} for holes	 100 100	 C/m^3 C/m^3
Detrapping barrier heights W_{tre} for electrons W_{trh} for holes	 0.96 0.99	 eV eV

It is well known that temperature can have a great impact on charge injection at the interface and charge transport inside the dielectrics [14]. When a current flows in the core of a cable, the heat generated from the conductor due to the Joule heating effect transfers into the cable insulation and outer screen gradually. In previous model [10], the temperature gradient across the insulation is considered as being under the steady state, which is different from that of a practical HVDC cable operation. Therefore, the transient changing of temperature gradient should be taken into account, in order to simulate charge behaviors under more realistic situations. In this paper, a DC current of 250A and 350A is applied to the cable core, which can stabilize temperature gradients of ~10°C and ~20°C across the insulation respectively after 2 hours heating. Based on the time dependent heat transfer equation shown as following, the temperature distribution across the insulation at each time step could be obtained.

$$\rho_d C_p \frac{\partial T}{\partial t} = \nabla \cdot (k \nabla T) + Q \quad (11)$$

where ρ_d is the material density; C_p is the heat capacity at constant pressure; k is the thermal conductivity; Q is the heat generated from the conductor, of the form:

$$Q = \frac{I^2 R_{dc}}{A} \quad (12)$$

where A is the cross section area of the conductor; I is the DC current. The boundary condition is set to be convective heat flux at the outer surface of insulator.

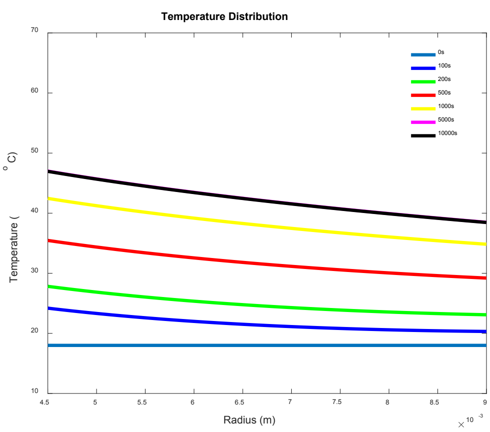

(a) 250A current

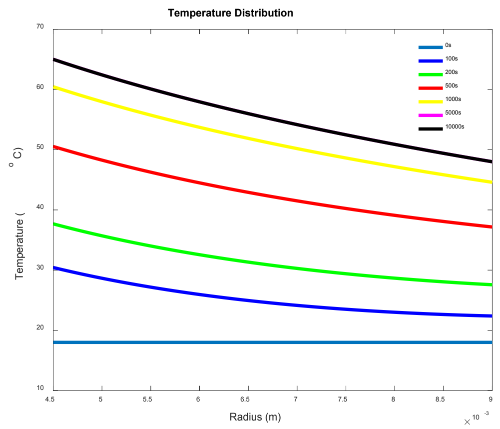

(b) 350A current

Fig. 3: The temperature distribution across the insulation with a current (a) 250 A and (b) 350 A flowing in the core of cable.

Figure 3 shows the transient temperature gradient profiles across the cable insulation with different values of current flowing in the conductor. It is clear to see that the temperature distribution seems to be stationary after 5000s in both cases. Here, we aim to analyse the space charge behaviour of the developed cylindrical model, namely the impact of the transient changing of temperature gradient.

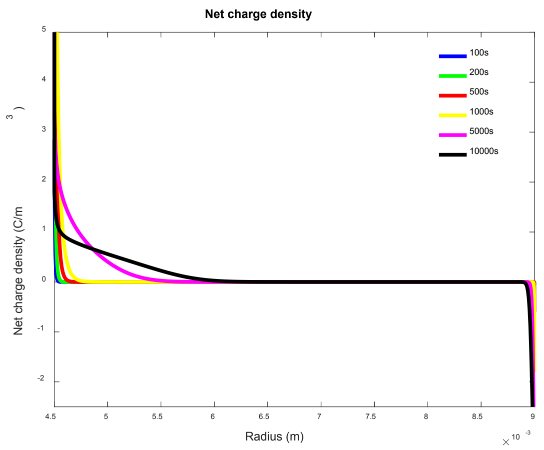

(a) 250A current

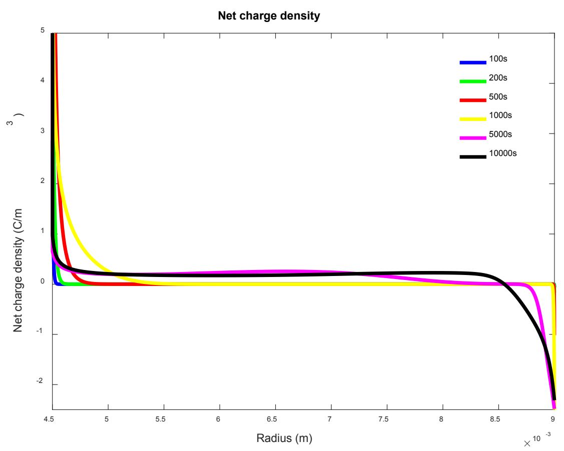

(b) 350A current

Fig. 4: The simulated space charge density profiles in cylindrical geometry for different polarization times. Applied voltage 90kv, with a current (a) 250 A and (b) 350A flowing in the core of cable.

The first objective is to compare the simulated results of the model for a 250A current and a 350A current flowing in the core of cable. The simulated charge densities for different polarization times are shown in Figure 4. After the application of voltage, positive and negative charge carriers are injected from the electrodes, and penetrate into the insulator. It should be noted that the y-axis has been truncated in Figure 4 in order to observe the movements of charges clearly. In the first case, the holes and electrons seem to remain in the vicinity of both electrodes respectively during first 500s. At 1000s, since the temperature increasing near the anode, the mobility of holes near the anode becomes higher, hence, holes can move into the bulk gradually. Compared with the first case, when the current flowing in the conductor changes from 250A to 350A, it can generate nearly twice as much heat as before. The temperature distribution across the insulation increases more significantly, thus enhancing the charge injection and mobility. In this situation, the amount of charge carriers is larger, and additionally, holes and electrons can penetrate deeper into the bulk. After 10000s, the space charge density seems to be stationary. The bulk is clearly charged positively, and only a small amount of electrons is observed close to the outer electrode.

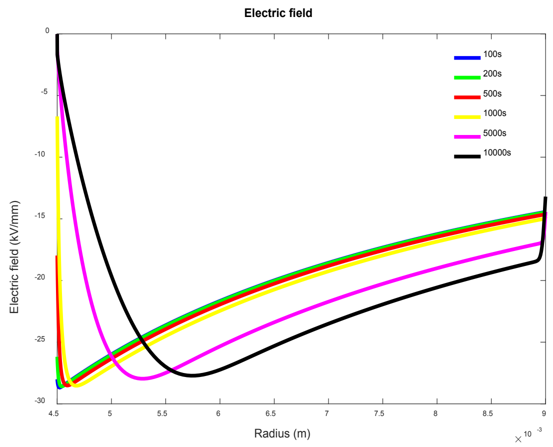

(a) 250A current

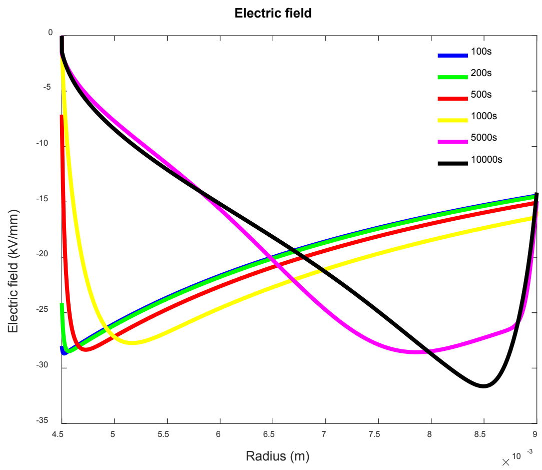

(b) 350A current

Fig. 5: The electric field distribution for different polarization times with a current (a) 250 A and (b) 350 A flowing in the core of cable.

The electric field distributions in the insulation as a function of time calculated with this model are shown in Figure 5. With the stressing time increasing, the presence of homocharges can decrease the electric field at the inner electrode gradually, leading to an approximately non-injection electrode at last. Compared with the 250A case, it can be seen that the maximal electric field location changes with time from the inner electrode to the outer electrode more obviously, and the value of the maximal electric field is higher too. This can be explained by the space charge behaviour shown in Figure 4. This reversing of position of the maximal field, named stress inversion phenomenon, has already been observed experimentally by space charge measurements on MV cables [5]. At 10000s, the maximal electric field reaches about 32.5kV/mm, and this phenomenon has already been observed in literature [15].

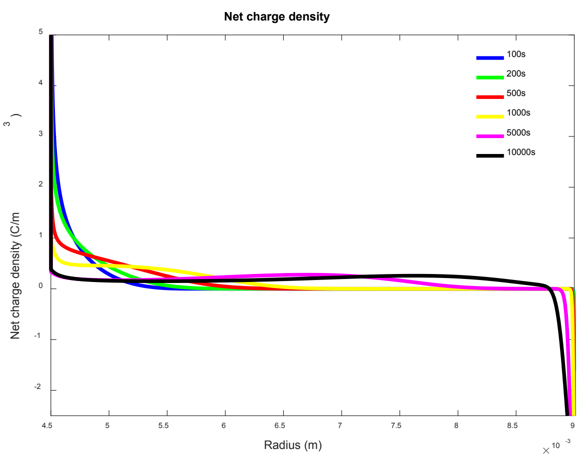

Fig. 6: The simulated space charge density profiles in cylindrical geometry with a steady temperature gradient across the insulation.

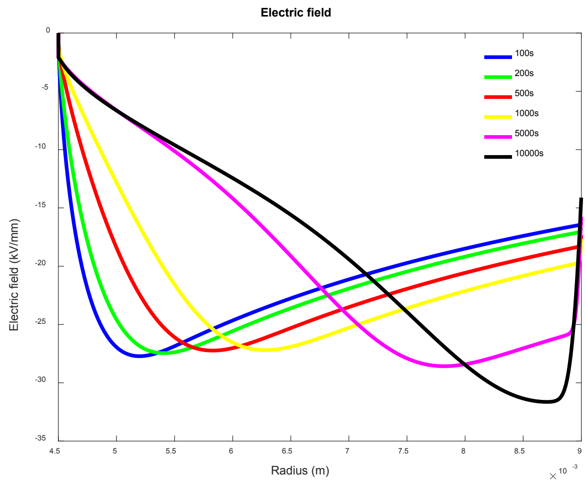

Fig. 7: The electric field distributions in cylindrical geometry with a steady temperature gradient across the insulation.

For the comparison, a steady temperature gradient across the insulation is carried out. The inner temperature is 65°C and the outer temperature is 45°C, which is similar with the stationary state of a 350A current flowing in the core of cable. The simulation results are shown in Figures 6 and 7. Compared the results of the model with a steady temperature gradient and the present model with a transient temperature gradient, we can observe that the penetration of charge carriers is not as deep as before during the first 1000s. However, the space charge distributions of both case are comparable after 5000s. This is because the temperature distributions of both case are similar, and thus leading to comparable charge mobility and injection. Additionally, unlike with a steady temperature gradient, the shifts of the maximal electric field location in the insulation is relatively slow with this transient temperature distribution in first 1000s. However, it shifts quickly in rest time since the correspond charge movement being accelerated.

Finally, the model can be used to simulate the space charge behavior in the cable geometry insulation (LDPE) with a transient temperature gradient across the insulation, and it is able to reproduce characteristic features that are observed experimentally for a cable geometry [16].

CONCLUSION

Based on the previous study on numerical space charge modelling, a modified bipolar charge transport model has been applied to simulate space charge behaviour in a cable geometry insulation (LDPE). A threshold electric field has been introduced into the model to redefine the charge injection from the electrodes. A transient temperature distribution calculated by heat diffusion has been applied across the insulation in the model, in order to present the space charge profiles in practical application cases. The simulated results show the thermal field can have a great impact on the space charge behaviour and electric field distribution. Additionally, it shows the necessity to consider the thermal transient when compared with results of a steady temperature gradient. This model can reproduce some specific features that observed experimentally on the MV size cable, such as the stress inversion phenomenon.

Optimizations still need to be made on the model parameters to reproduce the space charge behaviour in a XLPE material.

REFERENCES

[1] G. Chen, M. Hao, Z. Xu, A. Vaughan, Cao, Junzheng, and H. Wang, 2015, "Review of High Voltage Direct Current Cables," *10 Csee J. Power Energy Syst.*, vol. 1, no. 2, pp. 9–21.

[2] H. Ghorbani, M. Jeroense, C.-O. Olsson, and M. Saltzer, 2014, "HVDC cable systems—highlighting extruded technology," *IEEE Trans. Power Deliv.*, vol. 29, no. 1, pp. 414–421.

[3] T. L. Hanley, R. P. Burford, R. J. Fleming, and K. W. Barber, 2003, "A general review of polymeric insulation for use in HVDC cables," *IEEE Electr. Insul. Mag.*, vol. 19, no. 1, pp. 13–24.

[4] X. Wu, G. Chen, A. E. Davies, R. N. Hampton, S. J. Sutton, and S. G. Swingler, 2001, "Space charge measurements in polymeric HV insulation materials," *IEEE Trans. Dielectr. Electr. Insul.*, vol. 8, no. 4, pp. 725–730.

[5] M. S. Khalil, 1997, "International research and development trends and problems of HVDC cables with polymeric insulation," *IEEE Electr. Insul. Mag.*, vol. 13, no. 6, pp. 35–47.

[6] A. Vazquez, G. Chen, A. E. Davies, and R. Bosch, 1999, "Space charge measurement using pulsed electroacoustic technique and signal recovery," *J. Eur. Ceram. Soc.*, vol. 19, no. 6, pp. 1219–1222.

[7] S. Le Roy, P. Segur, G. Teyssedre, and C. Laurent, 2004, "Description of bipolar charge transport in polyethylene using a fluid model with a constant mobility: model prediction," *J. Phys. D. Appl. Phys.*, vol. 37, no. 2, pp. 298–305.

[8] G. Chen and S. H. Loi, 2005, "Space charge modelling in solid dielectrics under high electric field based on double charge injection model," *MRS Online Proc. Libr. Arch.*, vol. 889.

[9] S. Le Roy, G. Teyssedre, C. Laurent, G. C. Montanari, and F. Palmieri, 2006, "Description of charge transport in polyethylene using a fluid model with a constant mobility: fitting model and experiments," *J. Phys. D. Appl. Phys.*, vol. 39, no. 7, p. 1427.

[10] S. Le Roy, G. Teyssedre, and C. Laurent, 2016, "Modelling space charge in a cable geometry," *IEEE Trans. Dielectr. Electr. Insul.*, vol. 23, no. 4, pp. 2361–2367.

[11] K. C. Kao, 2004, *Dielectric phenomena in solids*. Academic press.

[12] S. Le Roy, F. Baudoin, V. Griseri, C. Laurent, and G. Teyssedre, 2010, "Charge transport modelling in electron-beam irradiated dielectrics: a model for polyethylene," *J. Phys. D. Appl. Phys.*, vol. 43, no. 31, p. 315402.

[13] G. C. Montanari, G. Mazzanti, F. Palmieri, A. Motori, G. Perego, and S. Serra, 2001, "Space-charge trapping and conduction in LDPE, HDPE and XLPE," *J. Phys. D. Appl. Phys.*, vol. 34, no. 18, p. 2902.

[14] G. Teyssedre and C. Laurent, 2005, "Charge transport modeling in insulating polymers: From molecular to macroscopic scale," *IEEE Trans. Dielectr. Electr. Insul.*, vol. 12, no. 5, pp. 857–874.

[15] D. Fabiani *et al.*, 2008, "HVDC cable design and space charge accumulation. part 3: effect of temperature gradient," *IEEE Electr. Insul. Mag.*, vol. 24, no. 2, pp. 5–14.

[16] R. Bodega, 2006, "Space charge accumulation in polymeric high voltage DC cable systems," Ph.D. degree thesis, Delft University of Technology.